Potential transport pathways of terrigenous material in the Gulf of Papua

Timothy R. Keen,[1] Dong Shan Ko,[1] Rudy L. Slingerland,[2] Shelley Riedlinger,[1] and Peter Flynn[1]

Received 6 December 2005; revised 18 January 2006; accepted 27 January 2006; published 25 February 2006.

[1] This work discusses potential transport pathways of terrigenous material in the Gulf of Papua (GoP), New Guinea, using Lagrangian tracers as proxies for clay minerals and finer particles. The tracers are transported by currents from the East Asia Seas implementation of the Navy Coastal Ocean Model. The results suggest that clay minerals input from rivers along the northwest coast of the GoP accumulate on the inner shelf with high concentrations near the mouth of the Fly and Purari Rivers. Finer particles, which are also representative of dissolved metals, are transported eastward along the GoP coast into the Solomon Sea as well as into the Torres Strait to the west. The results also suggest that some finer particles are entrained by eddies within the northern Coral Sea. These results are in qualitative agreement with observations from the region. **Citation:** Keen, T. R., D. S. Ko, R. L. Slingerland, S. Riedlinger, and P. Flynn (2006), Potential transport pathways of terrigenous material in the Gulf of Papua, *Geophys. Res. Lett.*, *33*, L04608, doi:10.1029/2005GL025416.

1. Introduction and Background

[2] The flux of particulate and dissolved material from New Guinea is very high [*Milliman et al.*, 1999; *Martin et al.*, 2000] and it thus serves as an excellent location to study the dispersal of terrigenous material into the ocean. The Gulf of Papua (GoP) (Figure 1) is receiving a substantial portion of this flux, as evidenced by its actively prograding clinoform [*Milliman et al.*, 2004]. The biogeochemical processes that determine the fate of terrigenous sediment within the GoP have been examined by numerous workers [see *Aller et al.*, 2004] as has the distribution of trace metals [*Apte and Day*, 1998; *Haynes and Kwan*, 2002]. These studies indicate that terrigenous material is transported by both coastal and deep-water currents.

[3] The physical oceanography of the GoP has been described in several studies [*Wolanski et al.*, 1984, 1995, 1999]. The Coral Sea Coastal Current (CSCC) forms a clockwise gyre that is strongest during the trade-wind season. Across-isobath tidal currents reach 1 m s^{-1} in response to water level fluctuations of 1–5 m at the mouth of the Fly River. Sub-tidal along-shelf currents of 0.1 m s^{-1} are coherent with the wind at periods of about 10 days on the inner shelf, whereas low-frequency currents within the mixed-layer are generally to the southwest. Some Fly River plume water may infrequently enter the Torres Straits because of sub-tidal water elevation differences between the GoP and the Arafura Sea. Modeling studies have been used in conjunction with measurement programs to elucidate dispersal mechanisms for noncohesive sediments in the GoP [*Wolanski et al.*, 1984, 1995; *Hemer et al.*, 2004].

[4] This study complements earlier work by examining the dispersal of dissolved and fine-grained suspended terrigenous material within the GoP for a year-long interval using a combination of hydrodynamic and Lagrangian tracer modeling. Furthermore, because of the large model domain used in this study, we are able to study the impact of large-scale flows on transport patterns without imposing artificial boundary conditions. The use of tracers to examine complex multidisciplinary problems in oceanography has led to understanding the behavior of both suspended and dissolved constituents in a range of ocean environments. [*Nakano and Povinec*, 2003; *McManus and Prandle*, 1997; *Tomczak and Herzfeld*, 1998]. Remobilization processes such as resuspension by waves have been examined by *Hemer et al.* [2004] and are not included in this study.

2. Hydrodynamic Simulations

2.1. The EAS16 Model

[5] The Navy Coastal Ocean Model (NCOM) is a three-dimensional primitive equation hydrodynamic model [*Morey et al.*, 2003]. Regional circulation during 2003 is simulated using the East Asian Seas implementation of NCOM (EAS16) with a horizontal cell size of 1/16° (Figure 1). The model assimilates monthly mean discharges for 51 rivers, synthetic temperature and salinity profiles, and altimetry. Surface boundary conditions consist of heat fluxes, precipitation, surface pressure, and wind stresses from an operational weather model (Navy Operational Global Atmospheric Prediction System). The open boundary conditions include sea surface elevation, transport, temperature, salinity and currents provided by the global NCOM model.

2.2. Circulation Within the Gulf of Papua

[6] The typical surface circulation from the EAS16 model during the northwest monsoon (Figure 2a) reveals the clockwise flow of the CSCC and a weak southward flow ($\sim$0.1 m s^{-1}) on the northwest shelf as reported by *Wolanski et al.* [1995]. The currents at the entrance to Torres Strait have not been reported for the monsoon but the predicted surface currents of approximately 0.4 m s^{-1} are probably high, based on observed oceanographic features [*Wolanski et al.*, 1984]. The relative magnitudes and directions, which are correct, reveal highly variable flow due to uncorrelated sea level fluctuations within the GoP and Arafura Sea.

[1]Naval Research Laboratory, Stennis Space Center, Mississippi, USA.
[2]Department of Geosciences, Pennsylvania State University, University Park, Pennsylvania, USA.

0094-8276/06/2005GL025416$05.00

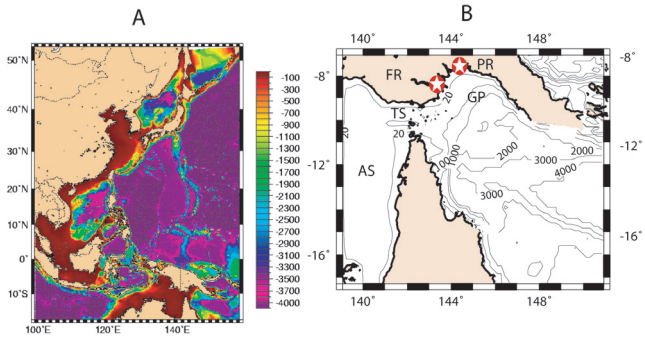

Figure 1. (a) Bathymetry used for the EAS16 model. The grid is approximately 1/16° with a horizontal resolution of 6–9 km. The box indicates the location of Figure 1b. (b) Detailed view of the Gulf of Papua and northern Coral Sea. Key: FR = Fly River; PR = Purari River; TS = Torres Straits; AS = Arafura Sea; GP = Gulf of Papua. The stars indicate where tracers are released.

Predicted surface currents of 0.1–0.2 m s^{-1} are eastward along the northeast coast of the GoP while bottom currents (Figure 2b) are on the order of 0.01 m s^{-1}. Bottom flow varies in direction because of the variable winds during the northwest monsoon.

[7] During the southeast trade-wind season, the surface currents on the shelf near the Fly River vary from west to southwest with speeds of 0.1–0.2 m s^{-1} (Figure 3a), whereas bottom currents of less than 0.1 m s^{-1} are predominantly southwest (Figure 3b) but with more variability than at the surface. The surface flow along the northern coast is weak and variable. Uniformly southeast surface currents near the northeast coast reach 1 m s^{-1} and the bottom flow is nearly aligned with surface flow. These results are consistent with observations [*Wolanski et al.*, 1995]. The modeled CSCC forms a closed clockwise loop during the trade-wind season but it has less impact on bottom flow at the shelf break than during the monsoon. The predicted flow into Torres Strait is higher than observed [*Wolanski et al.*, 1999] because the frictional effects of several large reefs within the northern Great Barrier Reef are absent in the EAS16 model.

3. Tracer Simulations

3.1. The Particle Tracking Model

[8] The particle tracking model uses three-dimensional current fields (u,v,w) and Gaussian random-walk dispersion [*Lu et al.*, 2002]. A particle's location (x,y,z) after a time step Δt is given by:

$$x_{t+1} = x_t + (u \cdot \Delta t) + (\Delta D_{LT} \cdot u/s) + (\Delta D_{LT} \cdot v/s) + \Delta D_{H0} \quad (1)$$

$$y_{t+1} = y_t + (v \cdot \Delta t) + (\Delta D_{LT} \cdot v/s) + (\Delta D_{LT} \cdot u/s) + \Delta D_{H0} \quad (2)$$

$$z_{t+1} = z_t + (w \cdot \Delta t) + \Delta D_{V0} \quad (3)$$

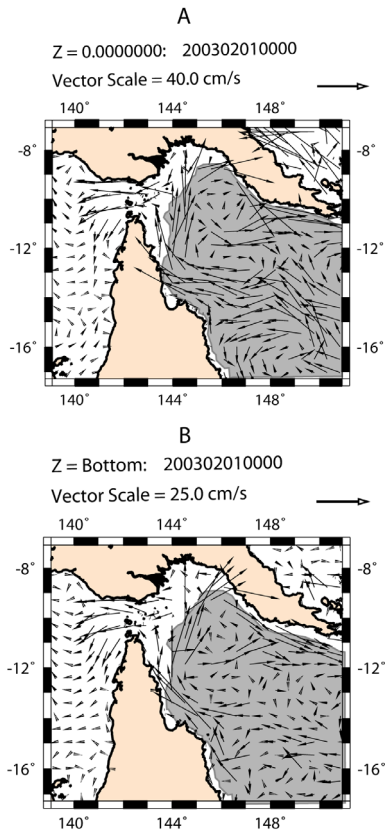

Figure 2. Currents predicted by the EAS16 model during the northwest monsoon period in the Gulf of Papua. (a) Surface currents. (b) Bottom currents. Depths below 100m are shaded.

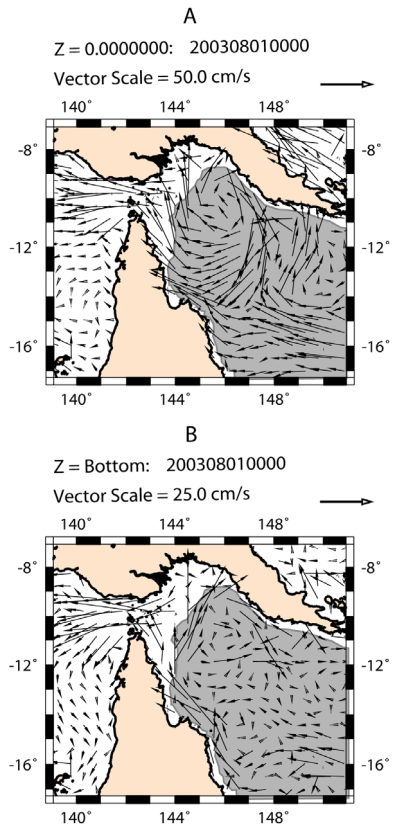

Figure 3. Currents predicted by the EAS16 model during the southeast trade wind period in the Gulf of Papua. (a) Surface currents. (b) Bottom currents. Depths below 100 m are shaded.

where: u = x-directed velocity; ΔD_{LT} = horizontal dispersion; s = current speed; v = y-directed velocity; ΔD_{H0} = neutral horizontal dispersion; ΔD_{V0} = neutral vertical dispersion; w = vertical velocity. The dispersion terms are given by:

$$\Delta D_{LT} = (6 \cdot K_{D1} \cdot \Delta t)^{0.5} \bullet \mathrm{RAND}^{1}_{-1} \quad (4)$$

$$\Delta D_{H0} = (6 \cdot K_{D2} \cdot \Delta t)0.5 \bullet \mathrm{RAND}^{1}_{-1} \quad (5)$$

$$\Delta D_{V0} = (6 \cdot K_{DV} \cdot \Delta t)0.5 \bullet \mathrm{RAND}^{1}_{-1} \quad (6)$$

where K_{D1}, K_{D2}, and K_{DV} are dispersion coefficients with values of 0.002, 0.002, and 0.0002 m^2/s, respectively. The dispersion terms are randomized for fractional values from -1 to 1 using the RAND^{1}_{-1} term, which has a Gaussian distribution. Particles are introduced at specified points using a fixed production rate of 2 particles per day. As a particle settles through the water column, equations (1)–(6) are solved at its new level before the settling velocity is applied. When the particle reaches the bottom it is deposited and can not be resuspended.

[9] Terrigenous input to the GoP is simulated using tracers with settling velocities of 10^{-5} m s^{-1} and 10^{-6} m s^{-1}. The faster-settling particles used in this study are more representative of natural flocculated particles [*Fugate and Friedrichs*, 2002] whereas the slower settling particles are included to represent unflocculated clay particles, woody debris, plankton, and dissolved substances.

3.2. Potential Transport Paths

[10] The tracer particles are released at two locations along the northwest coast of the GoP (see Figure 1b). The southern release point is at the mouth of the Fly River and the northern is west of the Purari River in an area with several sources of fresh water. These will be referred to as Purari particles. The heavier particles (indicated by yellow circles in Figure 4) settle near the sources but the Purari particles are more widely dispersed because of the stronger and more uniform currents along the northwest coast. The coastal currents transport the lighter particles eastward, such that Fly and Purari particles become mixed along the northern coast. Some of the Purari particles are transported as far as 149° East. These transport pathways persist until mid-March.

[11] The transition to the trade wind season occurs in March and April, by which time the lighter particles from the Fly River have reached the Purari but with an offshore displacement. By mid-March the coastal currents become westward at both rivers in response to early intensification of the southeast trade winds. The potential transport paths develop a stronger offshore component and the lighter particles reach the 20 m isobath. Eastward transport along the coast ceases by April but some of the lighter particles are entrained by eddies and transported beyond the shelf break. Some of these particles are then transported eastward in the CSCC. The weakening of the eastward coastal current is accompanied by an increase in deposition of lighter particles along the northeast coastline.

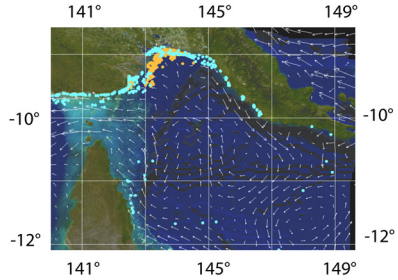

Figure 4. The distribution of particles after one year of integration. Topography is overlaid on model results using MODIS imagery. The yellow particles represent clay minerals and the blue represent finer particles.

[12] The trade wind circulation pattern becomes well established by May and lighter particles from the Fly River enter the Torres Strait along its northern boundary. Note, however, that none of the heavier particles enter the strait. As the trade-wind season continues, transport of lighter particles through the strait becomes more episodic in response to sea level variations within the GoP and the Arafura Sea. Eastward transport of Purari particles continues because of the persistent CSCC flow and these particles are entrained in eddies within the northern Coral Sea. The heavier particles from both sources are deposited very near the coast because of the westward and southwestward shelf flow.

4. Discussion and Conclusions

[13] The final particle distribution reveals transport paths for the faster settling particles, representing clay minerals, that are confined to the inner shelf (yellow circles in Figure 4). These potential transport paths are in agreement with field studies, which show high sedimentation rates on the inner shelf [*Walsh et al.*, 2004] and very little sediment transport into Torres Strait [*Wolanski et al.*, 1999]. Thus, it appears that clays are stored on the inner shelf along with the coarser silts and sands before being resuspended and transported to the clinoform face. Eastward transport of clays could have contributed to development of a clinoform within the northeastern GoP [*Droxler et al.*, 2004].

[14] The lighter particles represent river input of unflocculated clay minerals, CDOM, dissolved metals, and woody material. These particles are widely dispersed (blue circles in Figure 4). Their distribution is consistent with transport of lobster larvae by eddies within the northern Coral Sea [*Dennis et al.*, 2001]. Their transport into the Torres Straits is in agreement with measurements of dissolved metals [*Haynes and Kwan*, 2002; *Apte and Day*, 1998]. The potential transport pathways of dissolved material into the GoP and Solomon Sea to the east are also consistent with observations [*Milliman et al.*, 1999; *Martin et al.*, 2000].

[15] **Acknowledgments.** T. R. Keen and R. L. Slingerland gratefully acknowledge the support of the National Science Foundation, Award 0305699. This work was also supported by the Office of Naval Research through the Naval Research Laboratory 6.1 Core program.

References

Aller, R. C., A. Hannides, C. Heilbrun, and C. Panzeca (2004), Coupling of early diagenetic processes and sedimentary dynamics in tropical shelf

environments: The Gulf of Papua deltaic complex, *Cont. Shelf Res.*, *24*, 2455–2486.

Apte, S. C., and G. M. Day (1998), Dissolved metal concentrations in the Torres Strait and Gulf of Papua, *Mar. Pollut. Bull.*, *36*, 298–304.

Dennis, D. M., C. R. Pitcher, and T. D. Skewes (2001), Distribution and transport pathways of *Panulirus oratus* (Fabricus, 1776) and *Panulirus* spp. larvae in the Coral Sea, *Australia, Mar. Freshwater Res.*, *52*, 1175–1185.

Droxler, A. W., G. R. Dickens, S. J. Bentley, L. C. Peterson, and B. N. Opdyke (2004), Neogene evolution of the mixed carbonate/siliciclastic margin of the Gulf of Papua: Preliminary results of spring 2004 PANASH cruise on the R/V *Melville*, *Eos Trans. American Geophysical Union*, *85*(47), Fall Meet. Suppl., Abstract OS44A-08.

Fugate, D. C., and C. T. Friedrichs (2002), Determining concentration and fall velocity of estuarine particle populations using ADV, OBS and LISST, *Cont. Shelf Res.*, *22*, 1867–1886.

Haynes, D., and D. Kwan (2002), Trace metals in sediments from Torres Straits and the Gulf of Papua: Concentrations, distribution and water circulation patterns, *Mar. Pollut. Bull.*, *44*, 1296–1313.

Hemer, M. A., P. T. Harris, R. Coleman, and J. Hunter (2004), Sediment mobility due to currents and waves in the Torres Strait–Gulf of Papua region, *Cont. Shelf Res.*, *24*, 2297–2316.

Lu, S., F. J. Molz, and G. J. Fix (2002), Possible problems of scale dependency in applications of the three-dimensional fractional advection-dispersion equation to natural porous media, *Water Resour. Res.*, *38*(9), 1165, doi:10.1029/2001WR000624.

Martin, C. E., B. Peucker-Ehrenbrink, and G. J. Brunskill (2000), Sources and sinks of unradiogenic osmium runoff from Papua New Guinea, *Earth Planet. Sci. Lett.*, *183*, 261–274.

McManus, J. P., and D. Prandle (1997), Development of a model to reproduce observed suspended sediment distributions in the southern North Sea using principal component analysis and multiple linear regression, *Cont. Shelf Res.*, *17*, 761–778.

Milliman, J. D., K. L. Farnsworth, and C. S. Albertin (1999), Flux and fate of fluvial sediments leaving large islands in the East Indies, *J. Sea Res.*, *41*, 97–107.

Milliman, J. D., N. W. Driscoll, R. Slingerland, J. Babcock, and J. P. Walsh (2004), Isotopic stage 3 deposition and stage 2 erosion of a clinoform in the Gulf of Papua: Regional tectonics versus eustatic sea-level change, *Eos Trans. AGU*, *85*(47), Fall Meet. Suppl., Abstract OS44A-05.

Morey, S. L., P. J. Martin, J. J. O'Brien, A. A. Wallcraft, and J. Zavala-Hidalgo (2003), Export pathways for river discharged fresh water in the northern Gulf of Mexico, *J. Geophys. Res.*, *108*(C10), 3303, doi:10.1029/2002JC001674.

Nakano, M., and P. P. Povinec (2003), Oceanic general circulation model for the assessment of the distribution of ^{137}Cs in the world ocean, *Deep Sea Res., Part II*, *50*, 2803–2816.

Tomczak, M., and M. Herzfeld (1998), Pollutant pathways between Muruoa and other Polynesian islands, based on numerical model trajectories, *Mar. Pollut. Bull.*, *36*, 288–297.

Walsh, J. P., C. A. Nittrouer, C. M. Palinkas, A. S. Ogston, R. W. Sternberg, and G. J. Brunskill (2004), Clinoform mechanics in the Gulf of Papua, New Guinea, *Cont. Shelf Res.*, *24*, 2487–2510.

Wolanski, E., G. L. Pickard, and D. L. B. Jupp (1984), River plumes, coral reefs and mixing in the Gulf of Papua and the northern Great Barrier Reef, *Estuarine Coastal Shelf Sci.*, *18*, 291–314.

Wolanski, E., A. Norro, and B. King (1995), Water circulation in the Gulf of Papua, *Cont. Shelf Res.*, *15*, 185–212.

Wolanski, E., S. Spagnol, B. King, and T. Ayukai (1999), Patchiness in the Fly River plume in Torres Strait, *J. Mar. Syst.*, *18*, 369–381.

P. Flynn, T. R. Keen, D. S. Ko, and S. Riedlinger, Naval Research Laboratory, Stennis Space Center, MS 39529, USA. (keen@nrlssc.navy.mil)

R. L. Slingerland, Department of Geosciences, Penn State University, University Park, PA 16802–2714, USA.